Mutational Analysis of the *Saccharomyces cerevisiae* Cytochrome *c* Oxidase Assembly Protein Cox11p

Graham S. Banting and D. Moira Glerum*

Department of Medical Genetics, University of Alberta, Edmonton, Alberta T6G 2H7, Canada

Cox11p is an integral protein of the inner mitochondrial membrane that is essential for cytochrome *c* oxidase assembly. The bulk of the protein is located in the intermembrane space and displays high levels of evolutionary conservation. We have analyzed a collection of site-directed and random *cox11* mutants in an effort to further define essential portions of the molecule. Of the alleles studied, more than half had no apparent effect on Cox11p function. Among the respiration deficiency-encoding alleles, we identified three distinct phenotypes, which included a set of mutants with a misassembled or partially assembled cytochrome oxidase, as indicated by a blue-shifted cytochrome aa_3 peak. In addition to the shifted spectral signal, these mutants also display a specific reduction in the levels of subunit 1 (Cox1p). Two of these mutations are likely to occlude a surface pocket behind the copper-binding domain in Cox11p, based on analogy with the *Sinorhizobium meliloti* Cox11 solution structure, thereby suggesting that this pocket is crucial for Cox11p function. Sequential deletions of the matrix portion of Cox11p suggest that this domain is not functional beyond the residues involved in mitochondrial targeting and membrane insertion. In addition, our studies indicate that Δ*cox11*, like Δ*sco1*, displays a specific hypersensitivity to hydrogen peroxide. Our studies provide the first evidence at the level of the cytochrome oxidase holoenzyme that Cox1p is the in vivo target for Cox11p and suggest that Cox11p may also have a role in the response to hydrogen peroxide exposure.

Cytochrome oxidase (COX) is the terminal electron acceptor of the mitochondrial respiratory chain, accepting electrons from cytochrome *c*, reducing oxygen to water, and contributing to the proton gradient used to generate ATP. The mammalian COX holoenzyme consists of 13 subunits, of which the 3 "catalytic core" subunits are encoded by the mitochondrial DNA, with the remaining subunits encoded by the nuclear genome (26). Genetic screens in yeast have identified at least two dozen additional genes (17, 28) that are involved in the correct translation, processing, membrane insertion, and assembly of the COX structural subunits, in addition to the synthesis and insertion of the prosthetic groups. Subunit 1 (Cox1p) contains two heme molecules (a and a_3), in addition to a single copper atom that constitutes the Cu_B site, while subunit 2 (Cox2p) binds two copper atoms to form the binuclear Cu_A center. Several proteins are required for the insertion of these copper atoms into COX—Cox17p, Sco1p, and Cox11p. Originally identified as a *pet* mutant with a specific defect in COX assembly, a *cox17* null mutant could be rescued by exogenous copper, suggesting a role in mitochondrial copper metabolism (7). Subsequently, *SCO1* and *SCO2* were found to act as high-copy-number suppressors of a *cox17* allele, suggesting a downstream role in the copper insertion pathway (8). *cox11* was also identified as a *pet* mutant with a specific defect in COX assembly (27). All three proteins have been shown to bind copper, albeit with different configurations (4, 18, 25).

Cox11p exists as a dimer and contains three essential cysteine residues (4). The solution structure of a bacterial Cox11 homolog suggests that two of these cysteine residues are directly involved in copper binding while the third may form a disulfide bridge linking two Cox11 monomers (1). Cox11p is an integral inner mitochondrial membrane protein with an N-in, C-out orientation (5, 16); all evolutionarily conserved residues in Cox11p are within the intermembrane space (IMS) domain, suggesting that this domain contains the functional portion of the molecule. Additional studies with *Rhodobacter sphaeroides* have revealed that Cox11p is required for the formation of the Cu_B and magnesium centers of bacterial COX (12). Recent studies have shown that recombinant Cox11p and Sco1p will accept copper atoms from Cox17p in vitro (13). In combination with other yeast genetic data, the current model for copper provision to COX involves a "bucket brigade," in which Cox17p passes copper to Cox11p and Sco1p, which subsequently insert these atoms into nascent Cox1p and Cox2p, respectively.

The present study involved the random and targeted mutagenesis of *Saccharomyces cerevisiae* Cox11p, in which 48 *cox11* alleles were generated in an effort to more precisely determine essential regions of the protein. Our study has revealed that many Cox11p residues conserved over evolution (including a residue within the copper-binding domain) tolerate severe amino acid changes with no effect on Cox11p function, while others are essential for Cox11p stability and/or function. Our results confirm that the matrix domain is not required for Cox11p function. A specific reduction in levels of Cox1p, compared to levels of both Cox2p and Cox3p, supports the role for Cox11p in the delivery of copper specifically to the Cu_B site of COX. This study also shows that *cox11* mutants display a specific sensitivity to hydrogen peroxide, suggesting a possible secondary role for Cox11p in oxidative stress responses.

* Corresponding author. Mailing address: Department of Medical Genetics, University of Alberta, 8-33 Medical Sciences Building, Edmonton, Alberta T6G 2H7, Canada. Phone: (780) 492-4563. Fax: (780) 492-1998. E-mail: moira.glerum@ualberta.ca.

TABLE 1. Yeast strains used in this study

Strain	Genotype	Source or reference
W303-1A	**a** *ade2-1 his3-1,15 leu2-3,112 trp1-1 ura3-1*	A. Tzagoloff[a]
W303-1A ρ⁰	**a** *ade2-1 his3-1,15 leu2-3,112 trp1-1 ura3-1*	This study
W303ΔCOX4	**a** *ade2-1 his3-1,15 leu2-3,112 trp1-1 ura3-1 COX4::URA3*	A. Tzagoloff
W303ΔCOX6	**a** *ade2-1 his3-1,15 leu2-3,112 trp1-1 ura3-1 COX6::URA3*	A. Tzagoloff
W303ΔCOX9	**a** *ade2-1 his3-1,15 leu2-3,112 trp1-1 ura3-1 COX9::HIS3*	A. Tzagoloff
W303ΔCOX11	**a** *ade2-1 his3-1,15 leu2-3,112 trp1-1 ura3-1 COX11::HIS3*	24
W303ΔCOX17	**a** *ade2-1 his3-1,15 leu2-3,112 trp1-1 ura3-1 COX17::TRP1*	6
W303ΔSCO1	**a** *ade2-1 his3-1,15 leu2-3,112 trp1-1 ura3-1 SCO1::URA3*	7

[a] Department of Biological Sciences, Columbia University, New York, N.Y.

MATERIALS AND METHODS

Strains. All *cox11* mutants were studied in the aW303ΔCOX11 background (*ade2-1 his3-11,15 leu2-3,112 trp1-1 ura3-1 cox11::HIS3*) (27). Other strains used in this study are listed in Table 1. Media and conditions for growth of yeast have been previously described (27).

Generation of mutants. *cox11* mutants were generated by random or site-directed mutagenesis with pCOX11/ST3 (1.2-kb BamHI/PstI fragment in YEp351) and pCOX11/ST3.5 (1.2-kb BamHI/PstI fragment in YCplac111) as templates, respectively. Site-directed mutants were generated with the QuikChange kit (Stratagene, La Jolla, CA) with overlapping primers containing the desired mutation. Deletions were generated in the same fashion, except that the mutagenic primers formed a "splint" surrounding the region to be deleted. Random mutants were generated by a PCR-based method with 120 μM manganese and 120 μM dITP (22). All alleles with a single point mutation were generated by site-directed mutagenesis, and alleles with multiple mutations were generated by random mutagenesis. All mutations were confirmed by automated sequencing on an Avant3100 (Applied Biosystems, Foster City, CA).

Miscellaneous methods. Yeast cells were transformed according to the method of Schiestl and Gietz (24). Following prototrophic selection, transformants were replica plated to YEPG (rich ethanol-glycerol [EG]) (22) and scored for respiratory growth. Each strain was purified and tested to confirm cosegregation of the respiratory phenotype with the leucine prototrophy conferred by the YCplac111 vector. Strains were grown in YPGal (rich galactose medium [Gal]) (22) to stationary phase for isolation of mitochondria, as previously described (7). Protein concentrations, COX activities, and mitochondrial cytochrome spectra were all measured by standard methods (7). Proteins were separated on 12% polyacrylamide gels and immunoblotted with antibodies specific to Cox1p, Cox2p, and Cox3p (Invitrogen, Burlington, Ontario, Canada), porin (1:10,000), or Cox11p (1:1,500), followed by horseradish peroxidase-conjugated anti-rabbit (BD Biosciences, Mississauga, Ontario, Canada) or anti-mouse (Sigma-Aldrich, Oakville, Ontario, Canada) antibodies at a concentration of 1:7,500. Densitometric analysis of Western blots was carried out with the ImageJ program (http://rsb.info.nih/ij/). ρ⁰ yeast strains were generated as described by Goldring et al. (10), and hydrogen peroxide sensitivity assays were performed as previously described (30).

RESULTS

Respiratory phenotypes encoded by *cox11* alleles. The biogenesis of COX is a complex process requiring the concerted actions of many proteins, including Cox11p, which is proposed to act in the pathway providing copper to an assembling COX apoenzyme. In spite of the potential involvement of *COX11* as a candidate for mutation in human COX deficiencies, the only evidence for its role in the formation of the Cu_B site comes from studies in the prokaryote *R. sphaeroides* (12). Although there has been an in-depth characterization of the copper-binding function of yeast Cox11p (4), little is known about the amino acid residues that are required for the protein to fulfill its proposed role in copper transfer to Cox1p. In order to determine which portions of Cox11p are important for its function, we used a combined random and site-directed muta-

genesis approach. An alignment of Cox11 proteins from 10 disparate species (Fig. 1) shows that conservation of Cox11p is confined to residues in the IMS domain, with little or no similarity within the predicted transmembrane (TM) helix or matrix domain. At the outset of this study, there was no structural information regarding Cox11p and therefore residues that were identical across all 10 species were targeted for mutagenesis. In each case, residues were changed to introduce an amino acid with properties dramatically different from those of the wild-type residue. Upon verification of the mutant allele sequences, each allele was transformed into the *cox11* null mutant (27) on a CEN plasmid. Following prototrophic selection, each allele was scored for growth on EG (Fig. 1) and cosegregation of the leucine prototrophy and respiratory phenotype. Table 2 presents a list of the respiratory phenotypes observed, with growth rates compared to that of the wild-type strain (100%). Approximately half of the mutations generated had no discernible effect on Cox11p function despite the absolute conservation of the affected residues. It was notable that the F211A mutation, which affects the last amino acid in the CFCF copper-binding loop, had no impact on Cox11p function. Mutation of the three cysteine residues found in the IMS domain of the protein lead to complete respiratory deficiency (growth rate of 0), as demonstrated previously by Winge and coworkers (4).

We also analyzed a series of *cox11* random mutants that had been generated in an earlier phase of the project, along with three mutants from the G53 complementation group (28). The G53 alleles were amplified by PCR, sequenced, and subcloned into a CEN plasmid prior to transformation into aW303ΔCOX11. All of the random and G53 mutants contained two or more mutations, and we found that all of these mutants, with the exception of the E212G/M240K allele, have a complete, or almost complete, loss of Cox11p activity, as judged by their inability to grow on EG. Because we had noted that the D57V/L106P/S150P triple mutant could actually complement the *cox11* null mutant when expressed from a multicopy plasmid (data not shown), while the single-copy mutant is completely respiration deficient, we wondered which mutation(s) was responsible for the respiratory deficiency. We therefore used site-directed mutagenesis to generate all combinations of these three mutations. The D57V mutant displays a wild-type growth rate on EG, as does the S150P allele. By contrast, the mutant with L106P on its own had a compromised ability to respire (Table 2), growing at approximately one-quarter of the wild-type rate. Combining the D57V and L106P mutations does not appear to have a greater impact on Cox11p function

```
                                                                              ----    ----
human        MGGLWRPGWRCVPFCGWRWIHPGSPTRAAERVEPFLRPEWSGTGGAERGLRWLGTWKRCS   60
orangutan    MGGLWRPGWRRVAFCGWRWIHPGSPTRAAERVEPFLRPECSGTGGAGRGLRWLGTWKRCS   60
mouse        MGGLWCPGWRLVASCGRGWRQPGWSGRTVVNAELVLRPGWDGLGGAERGLRRLGTWKR-P   59
c.elegans    ------------------------------------------------------------    0
yeast        MIRICPIVRSKVPLLG----------TFLRSDSWLAPHALALRRAICKNVALRSYSVNS    49
s.meliloti   ------------------------------------------------------------    0
rhodobacter  ------------MPPPPPPSLARLHQR--LSLSLLRGR----SPPAAADAFLRR-----M    1
rice         ------SLARLHQR--LSLSLLRGR----SPPAAADAFLRR----GLASSA           41
arabidopsis  MSWSKACRGTRISSYLENLHRTSQYPRTILCSRYYTHGACKSNEHYLRSKRVFWGSSSSW   60
neurospora   ---------MSSMPRFVGRRAVAVQSFSQSASWACFSCRQEFQNQWRRQLSFDTEAPSAA   51

             Δ49-53    Δ54-63      Δ64-73       Δ74-83      Δ84-88    TM
human        LRARHPALQPPRRPKSSNPFTRAQEE-ERRRQNKTTLTYVAAVAVGMLGASYAAVFLYRL  119
orangutan    LGARHPALQPPRRHKNSNPFTRAQKE-EWRRRNKTTLTYVAAVAVGMLGASYAAVFLYRL  119
mouse        CGVRGPATQPPRRPRSSNPFQRAQED-EWRRRNKTVLTYVAAAVGMLGASYAAVFLYRL   119
c.elegans    ----------------------------------MSLVIVAIGCTFAAIFAYRI         20
yeast        EQPKHTFDISKLTRNEIQQLRELKRARERKFKDRTVAFYFSSVAVLFLGLAYAAVFLYRA  109
s.meliloti   --------------------------------------MVFLYDM                  7
rhodobacter  SLSPHQKTAG---------------------------GLVLVVAVMGAASFAAVFFYNW    33
rice         SSSSAAAAAVAAAAAGR-----------EKSSRRTLAYLLGVAAAMVGASYLRVFLYRK   91
arabidopsis  SLNSHSATAKSMLDSAHRQYSTHSPS---ETKSQKMLYYLTAVVFGMVGLTYAAVFLYRT  117
neurospora   SSDPRRKMTTAAQQQASGAKKQQSDRAWRWFSTEGASRRQQQQQTRSQSSRTGVSPEMER  111

                  VV           G         S          βa0    βa  P* K
human        YCQTGLGGSAVAGH----ASDKIENMVPVK----DRIIKISFNADVHASLQWNFRPQQT  171
orangutan    YCQTGLGGSAVAGH----ASDKIENMVPVK----DRIIKISFNADVHASLQWNFRPQQT  171
mouse        YCQTGLGGSAVAGH----SSDQIENMVPVK----DRVIKVTFNADVHASLQWNFRPQQT  171
c.elegans    FCEQSFGGLTQVAK----DFDKIANMKKCE----DRLIRVQFNSDVPSSMRWEFKPQQH   72
yeast        ICARGFGGIPITDR----RKFTDDKLIPVDT---EKRIRISFTSEVSQILPWKFVPQQR  162
s.meliloti   FCRVGYNGTTQRVE----QASDLIL---------DEKIKVTFDANVAAGLPWEFVPVQR   54
rhodobacter  FGRVGFAGTTAVAT----EAPAEVL---------DRTVKVRFDASREAGMPWEFRPLQR   80
rice         FCQATGYGGTVQRRE---SVEEKISRHARDGTTTSREIIVQFNADVADGMPWKFIPTQR  147
arabidopsis  FCQATGYGGTVQRKE---TVEEKIARHSESGTVTEREIIVQFNADVADGMQWKFTFTQR  173
neurospora   ICQTLGWGQPVRAHGAGGSDSDVDLAAKLEPVRDAKRMRVTFSASVSDVLPWKFVPQQR  171

             A βa'        βb        βc        βc'      βd  A  P*  βd' R
human        EIYVVPGETALAFYRAKNPTDKPVIGISTYNIVFFEAGQYFNKIQ-CFCFEQRLNPQLE  230
orangutan    EIYVVPGETALAFYRAKNPTDKPVIGISTYNIVFFEAGQYFNKIQQCFCFEQRLNPQLE  231
mouse        EIYVVPGETALAFYKAKNPTDKPVIGISTYNVFFEAGQYFNKIQ-CFCFEQRLNPQLE   230
c.elegans    EIYVHPGETALAFYTARNPTDKPIIGISSYNLTPFGEAAQYFNKIQ-CFCFEQKLAAGE  131
yeast        EVYVLPGETALAFYKAKNYSDKDIIQMATYSIAFGEAAQYFNKIQ-CFCFEQKLAAGE   221
s.meliloti   DIDVRIGETVQIMYRAKNLASTPTTQATFNVTPMAAGAYFNKVQ-CFCFTETTLEPGE   113
rhodobacter  EMKLKIGETGLAFYEAYNPTDRTVAQTASYNVTPDAAGGYFAIA-CFCFTEQVLAPGR   139
rice         EVKVKPGESALAFYTAENRSSAPITGVSTYNVAPMKAAIYFNKIQ-CFCFEQTLLPGIQ  206
arabidopsis  EVRVKPGESALAFYTAEKSSAPITGVSTYNVTPMKAGVYFNKIQ-CFCFEQRLPGIQ   232
neurospora   EVRILPGETALAFYTATMSDKDIIGVATYSVTPGQVAPYFSKIQ-CFCFEQRLNAGET  230

             βe   D     α         K        βf   T   R    A    L E  AAAAK# A
human        VDMPVFFYIDPEFAEDPRMIKVDLITLSYTFEAKEGHKLPVPGYN----------   276
orangutan    VDMPVFFYIDPEFAEDPRMIKVDLITLSYTFEAKEGHKLPVPGYNSSQQLSLPSKL--- 288
mouse        VDMPVFFYIDPEFAEDPRMIKVDLITLSYTFEAKEGHKLPVPGYN----------   275
c.elegans    VDLPVFFYIDPDYVNDPALEYLDSILSYTFEAKSGLKLPDP-FDPKNRPSIAPSPDKV  190
yeast        IDMPVFFFIDPDFASDPAMRNIDDIILHYTFRAHYGDGTAVSDSKKEPEMNADEKAASL  281
s.meliloti   MEMPVVFFVDPEIVKPVETQGIKTLTLSYTFYPREPSKPVAQVKAKAENKL-------  161
rhodobacter  VEMPVVFYVDPAIIDDPDGRYVRQITLSYTFHETALTEEQAALAAESATDVN-------  191
rice         IDMPVFFYIDPEFETDPRMDGINNLILSYTFKVNDS--------------         244
arabidopsis  IDMPVFFYIDPEFETDPRMDGINNLILSYTFKVSEENTTETVNNNNSVPVQETN----  287
neurospora   VDMPVFFYLDPDYLNDLNMKGIETVTLSYTFKAKYDDNGVLKGVPGAP----------  279

             RD    K        K#        G    F D           G
             W
human        ------------------
orangutan    ------------------
mouse        ------------------
c.elegans    PEATK------------- 195
yeast        ANAAILSPEVIDTRKDNSN 300
s.meliloti   ------------------
rhodobacter  ------------------
rice         ------------------
arabidopsis  ------------------
neurospora   ------------------
```
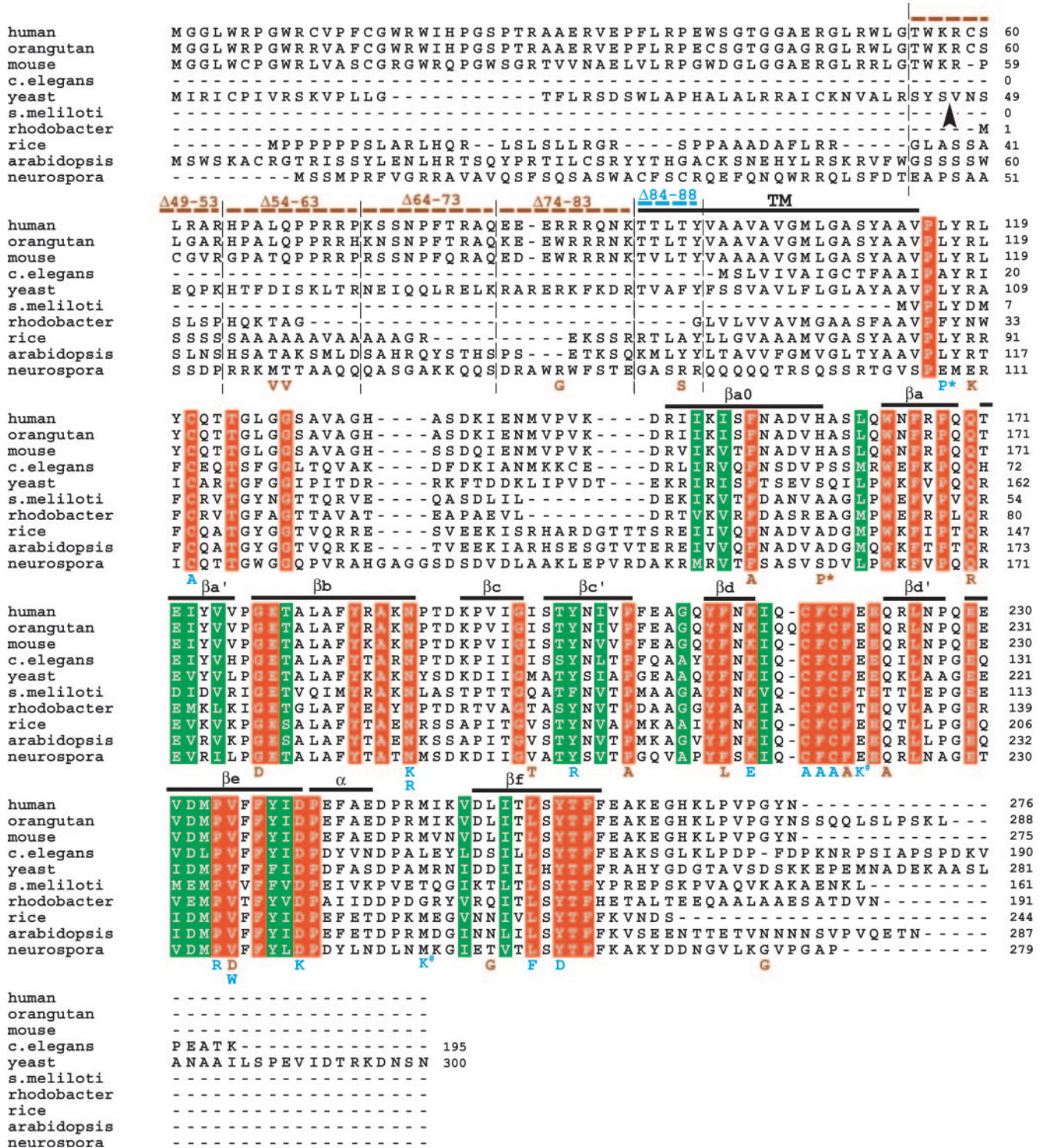
FIG. 1. Alignment of multiple Cox11p sequences from 10 disparate species with a summary of Cox11p mutations generated in yeast. ClustalX was used to align Cox11p sequences from 10 species. Residues identical across all 10 species are highlighted in red, while residues conserved across all 10 species are highlighted in green. The putative TM domain of the yeast sequence is shown overlined in black. The 10 β-strands assigned by Banci et al. (1) are overlined and labeled. The predicted MPP cleavage site for yeast Cox11p is denoted by the arrowhead. Point mutations generated in yeast Cox11p are shown below the alignment and are color coded as follows on the basis of the phenotypes they encode: brown, respiration competent; blue, respiration deficient (petite). Deletions generated in yeast Cox11p are shown above the alignment by dotted lines and are color coded as are the single-residue mutations. Symbols: *, mutations that synthetically interact to produce complete respiratory deficiency; #, mutations that produce a synthetic partial respiratory deficiency. The S. meliloti sequence represents only the soluble domain of Cox11.

TABLE 2. Summary of respiratory phenotypes of *coxII* alleles

Allele[a]	Growth on EG (%)[b]	Allele[c]	Growth on EG (%)[b]
Wild type	100	E212G/M240K[d]	60
C5R	100	D231K	60
D57V	100	R78G/F87S	50
I58V	100	L248F	50
R78G	100	Y250D	33
F87S	100	D57V/L106P	25
R108K/F203L	100	L106P	25
F145A	100	N38/G169D/K214E[d]	0
S150P	100	D57V/L106P/S150P	0
D57V/S150P	100	C111A	0
Q161R	100	L106P/S150P	0
M189T	100	G169D/E213G/D245G/D256G	0
Y192F	100	N180K	0
Y192H/E269G	100	N180R	0
P196A	100	G188D/A235D[d]	0
F211A	100	Y192R	0
Q214A	100	K205E	0
D245G	100	C208A	0
V226D	100	F209A	0
Δ49–53	100	C210A	0
Δ54–58	100	P225R	0
Δ59–63	100	V226W	0
Δ64–68	100	Δ84–88	0
Δ69–73	100	ΔCOX11	0
Δ74–78	100		
Δ79–84	100		
Δ44–53	100		
Δ54–63	100		
Δ64–73	100		
Δ74–83	100		

[a] Mutations that had no effect on respiration are listed in this column. Mutated residues are listed in order, from the N terminus to the C terminus.

[b] Growth rates were determined by replica plating strains to EG and checking growth at 30°C every 24 h. The growth rate of each mutant allele on EG is given as a percentage of that of the wild-type parent strain (100%), which grows to confluence on EG after 24 h.

[c] Mutations that compromised respiratory growth are listed in this column, in order of decreasing growth rate. Alleles encoding complete respiration deficiency (0% growth) are listed in order, from the N terminus to the C terminus.

[d] From the G53 complementation group (27).

than that already conferred by the L106P change (Table 2). However, combining L106P with S150P demonstrated a synthetic interaction, resulting in complete respiratory deficiency.

COX assembly mutants that display reduced respiratory growth typically possess residual COX activity that is proportional to their growth rate (22). We isolated mitochondria from the *cox11* mutant strains that displayed a respiratory deficiency phenotype and assayed their COX activities. As shown in Table 3 for a subset of *cox11* alleles, the mutants displayed residual COX activities that were commensurate with their growth rates on EG—those mutants that were completely respiration deficient had COX activity levels similar to that found with the *cox11* null strain. Given that an approximately 40% reduction in COX activity will still support respiratory growth that is indistinguishable from that seen with a respiratory competent strain (9), we also tested COX activity levels in several of our respiratory competent *cox11* mutant strains. The D57V and S150P mutants had COX activity levels that were 90% and 120%, respectively, of the wild-type levels (data not shown), supporting the notion that these mutations have no substantive impact on the ability of Cox11p to participate in the COX assembly process.

Cox11p has a novel surface pocket that is essential for its function. The solution structure for a Cox11 homolog from the bacterium *Sinorhizobium meliloti* was recently solved (1), and examination of the structure indicated the presence of a surface pocket in the protein that is situated behind the copper-binding loop and extends into the center of the β-barrel-like structure (Fig. 2A and B). We postulated that this pocket would be important for Cox11p function and modeled amino

TABLE 3. Summary of COX activities of mutants with selected *cox11* mutant alleles

Allele[a]	COX activity (μmol/min/mg)[b]
Wild type	1.83
ΔCOX11	0.02
D57V/L106P	0.10
L106P	0.16
C111A	0.02
Y192R	0.01
K205E	0.01
C208A	0.01
F209A	0.01
C210A	0.01
P225R	0.01
V226W	0.01
D231K	0.96
L248F	0.72
Y250D	0.22

[a] Alleles are listed in order, from the N terminus to the C terminus.

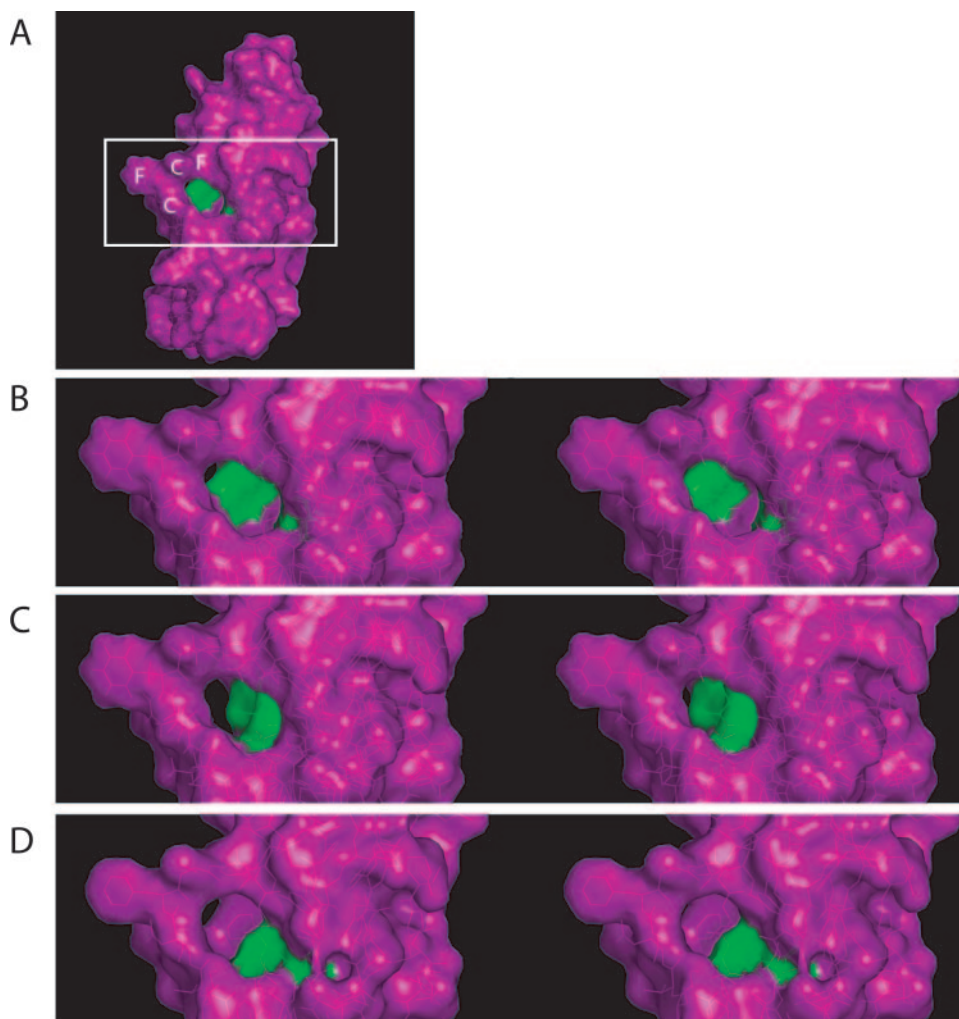[b] COX activity represents the mean of two determinations.

FIG. 2. Comparative stereo views of two *cox11* alleles generated based on molecular modeling of the *S. meliloti* Cox11 three-dimensional structure. (A) Model of *S. meliloti* Cox11 (Protein Data Bank code, 1SO9). The side chains of residues F84 (Y192 in yeast) and V118 (V226 in yeast) are shown in green. These residues border a pocket in the protein behind the CFCF copper-binding loop, which is labeled. The boxed region was used to generate stereo views. (B to D) Stereo views of the wild-type (B) and theoretical F84R (C) and V118W (D) *cox11* mutant alleles from *S. meliloti*. In panels C and D, only the mutated residue is green. Mutations were generated in 1SO9 with the Swiss Protein Data Bank viewer, followed by energy minimization. Stereo views were subsequently generated with Pymol.

acid changes in which the side chains of two separate residues would project into this pocket and partially occlude it. Two mutations in *S. meliloti* were chosen (F84R and V118W), and the corresponding changes were generated in the yeast Cox11p (Y192R and V226W) (Fig. 2C and D). Both of these alleles resulted in complete respiratory deficiency and loss of COX activity. We had already noted that mutants with either a Y192H or a V226D change had no adverse effect on respiration (Table 2)—neither of these changes appears to result in any occlusion of the pocket. Our results thus suggest that this previously unidentified surface pocket is essential for Cox11p function.

A subset of *cox11* mutants have a misassembled COX enzyme. Ablation of *COX11* in yeast results in loss of COX activity, along with loss of the cytochrome aa_3 spectral peak (603 nm) that is indicative of the amount of assembled COX holoenzyme (27). All of the yeast COX assembly null alleles studied to date are characterized by complete loss of COX assem-

bly, as typified by the loss of the 603-nm peak (21). In the last few years, a number of yeast mutants have been described that give rise to a COX "misassembly" phenotype. These mutants, which have been described for *SCO1* and *COX17*, are respiration deficient and lack COX activity, but in contrast to their respective null alleles, they display a cytochrome aa_3 spectral peak that is shifted to the blue range by several nanometers (6, 22). This shift is indicative of an abnormal environment for the heme a and a_3 molecules. In order to determine the effect of the *COX11* mutations on COX assembly per se, we analyzed the cytochrome spectra of detergent-solubilized mitochondrial extracts (Fig. 3). The mutant alleles fell into three broad categories: (i) mutants with complete respiratory deficiency and loss of the aa_3 peak, as exemplified by the C111A and K205E alleles; (ii) mutants characterized by complete respiratory deficiency with a reduced and blue-shifted aa_3 peak (Y192R and V226W); and (iii) mutants displaying partial respiratory deficiency (i.e., reduced growth on EG) with a reduced and blue-
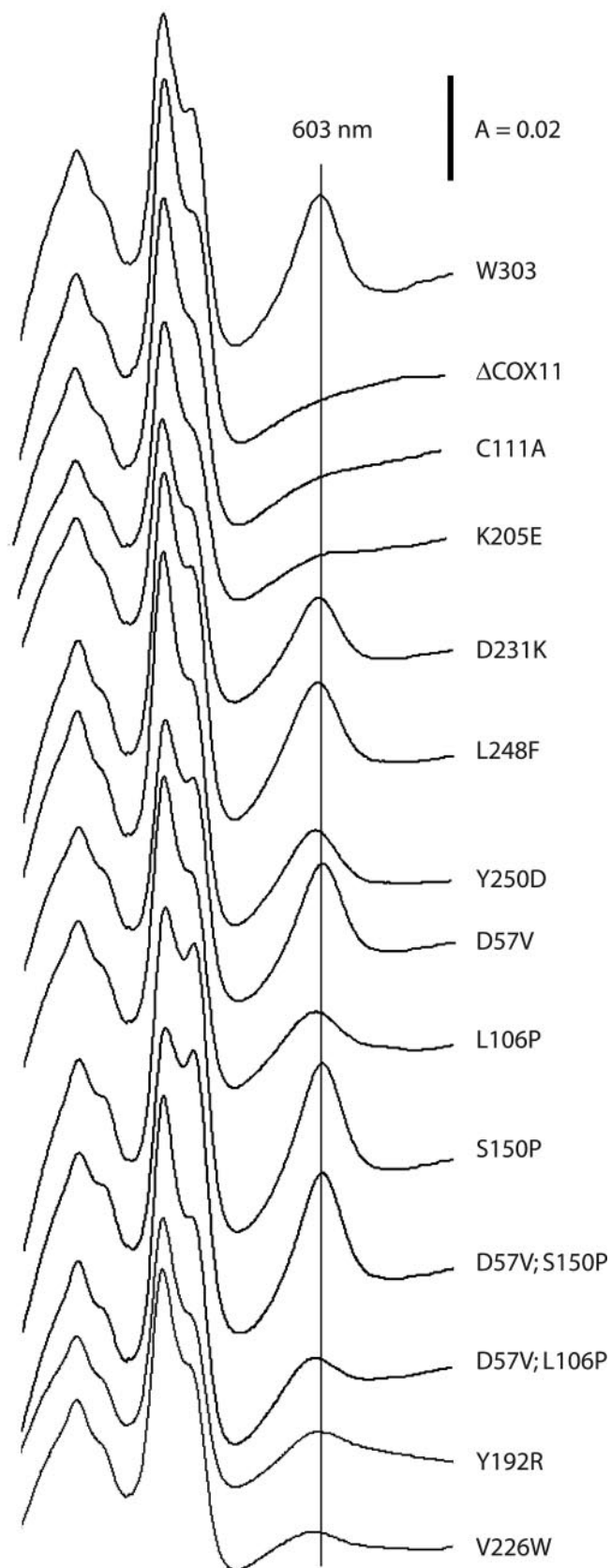
FIG. 3. Mitochondrial cytochrome spectra of *cox11* mutants fall into three categories. Mitochondria were solubilized in 1% deoxycholate, and

shifted cytochrome aa_3 absorption peak (L106P was representative of this category). The first group of mutants is similar to the null allele, lacking both a 603-nm peak and COX activity. Only two mutants fell into group 2, displaying a phenotype reminiscent of several *cox17* mutants we described previously (22). These group 2 mutants have a misassembled COX enzyme, given that they have no COX activity but still display a spectral signal in the vicinity of 603 nm. Perhaps the most interesting mutants fall into group 3 (L106P, D231K, L248F, and Y250D), which is characterized by residual respiratory growth and residual COX activity. However, these mutants are unique among known yeast COX assembly mutants in that their spectral peak is shifted 1 to 3 nm to the blue range from the normal 603 nm and that the peak is not reduced to the extent expected from their rates of growth on EG. Given that they have residual COX activity, the group 3 mutants likely produce a partially assembled COX enzyme. These group 3 mutants display a phenotype that has not been observed for any of the yeast COX assembly mutants described to date.

As discussed above, some of the single and double Cox11p mutations we examined did not give rise to respiratory deficiency. In order to ascertain whether some of these mutations might have a subtle effect on COX assembly, we also carried out cytochrome spectral analyses for mitochondria isolated from the D57V, S150P, and D57V/S150P mutants (Fig. 3). In each case, the mutant displayed the expected peak at 603 nm, with a magnitude indistinguishable from that of respiratory competent W303. Together with their wild-type COX activities (as discussed above), this further confirms that none of these mutations had any impact on Cox11p function.

A subset of *cox11* mutants are characterized by selectively reduced levels of Cox1p. In addition to the loss of COX activity and the cytochrome aa_3 spectral peak, COX assembly mutants are generally characterized by a loss of steady-state levels of the mitochondrially encoded subunits that form the catalytic core of COX (9). As with the cytochrome spectral profile, the only exceptions to this are a group of *sco1* and *cox17* mutants, which were shown to have a selective loss of Cox2p (6, 22). We therefore performed Western blot analysis to assess the levels of Cox1p, Cox2p, and Cox3p in mitochondrial extracts from our *cox11* mutants. All samples were also immunoblotted for Por1p, a mitochondrial porin, to ensure that any differences in protein levels did not arise from uneven loading of the gels. As shown in Fig. 4A, those mutants (group 3, above) that retained residual COX activity, with a shifted cytochrome aa_3 peak, had levels of all three mitochondrially encoded subunits that are similar to those seen with the wild-type parent strain, W303. Similarly, the mutants that did not have a respiratory defi-

the difference spectra of mitochondrial extracts reduced with sodium dithionite and oxidized with potassium ferricyanide are shown. Parent strain W303 displays a typical cytochrome aa_3 peak at 603 nm, which is denoted by the vertical line. The Δ*cox11* mutant and most of the respiration-deficient *cox11* mutants lack a peak at 603 nm. Several of the *cox11* allele mutants with partial respiratory deficiency display aa_3 peaks that are reduced and shifted 1 to 3 nm to the blue range. The Y192R and V226W alleles are the only complete respiration deficiency-encoding alleles for which an aa_3 peak is observed. Mutants are labeled according to the mutations they bear.
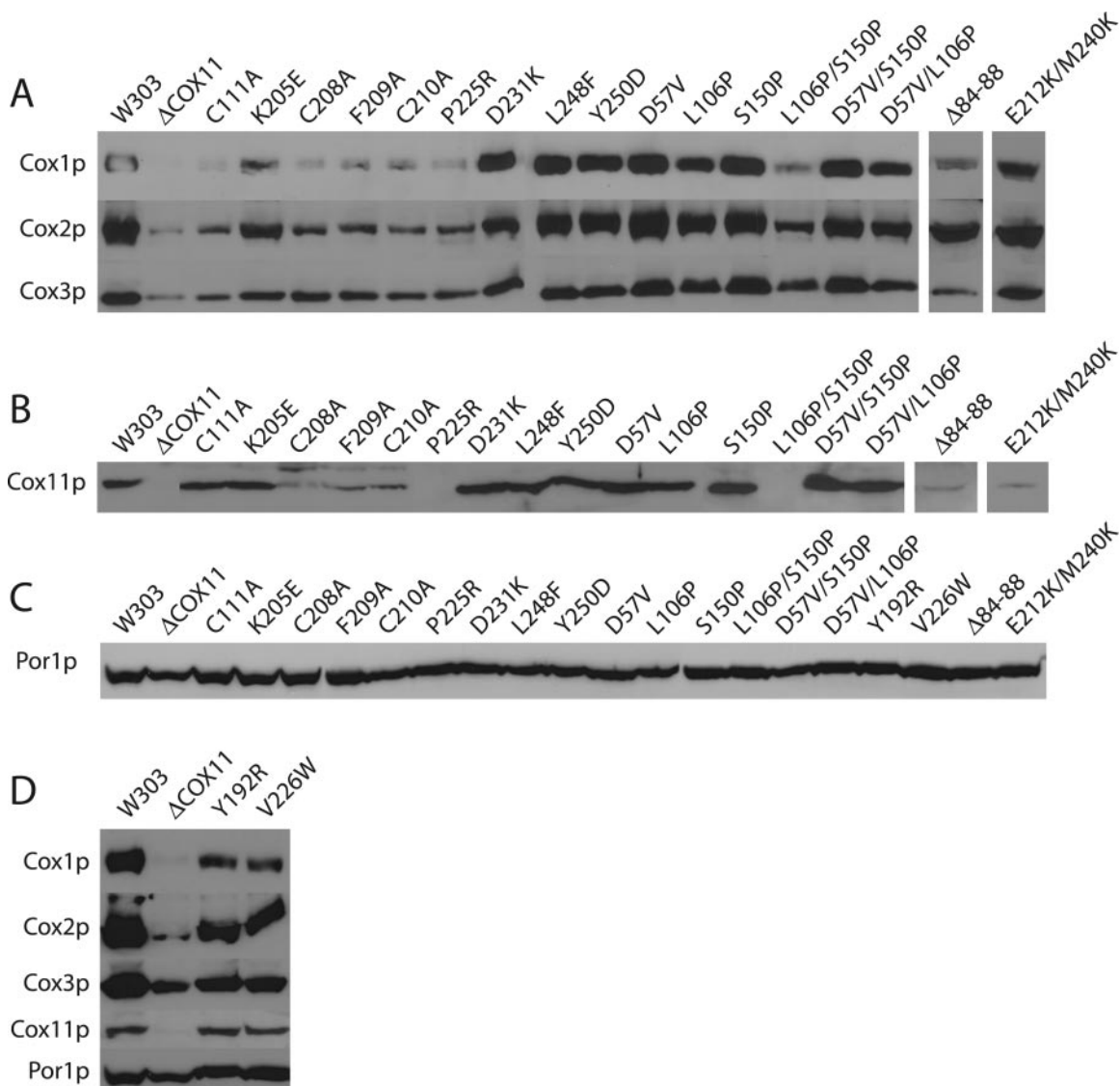
FIG. 4. Western blot analysis of Cox11p, Por1p, and COX catalytic core proteins from *cox11* alleles. Mitochondria were purified from strains expressing each *cox11* allele on a low-copy-number plasmid. Mitochondrial proteins (20 μg) were separated on 12% polyacrylamide gels and transferred to nitrocellulose membrane prior to probing with antibodies specific to Cox1p, Cox2p, Cox3p, Cox11p, and Por1p. (A) Steady-state levels of COX subunits 1, 2, and 3. Mitochondria from all mutants, except those with the Δ84-88 and E212K/M240K mutations, were electrophoresed and blotted together. The mutants with Δ84-88 and E212K/M240K were analyzed separately but with the same wild-type (W303) and null mutant (ΔCOX11) mitochondrial samples to allow comparison. (B) Steady-state levels of Cox11p were determined in the same experiment for all mutants except those with the Δ84-88 and E212K/M240K mutations, which were analyzed separately as described for panel A. Cox11p instability is observed in several of the complete respiratory deficiency-encoding alleles (C208A, F209A, C210A, P225R, L106P/S150P, and Δ84-88). (C) All samples were blotted for mitochondrial porin (Por1p) to ensure loading of uniform amounts of protein. (D) The two *cox11* mutants that result from occlusion of the pocket behind the copper-binding domain were analyzed for steady-state levels of Cox1p, Cox2p, Cox3p, Cox11p, and Por1p. The misassembled mutants (Y192R, V226W) have proportionally less Cox1p than Cox2p or Cox3p, with uniform levels of Por1p.

ciency also had wild-type levels of these three subunits. In contrast, those mutants that lacked a COX spectral signal (i.e., C111A) also had markedly decreased levels of Cox1p, Cox2p, and Cox3p, similar to those seen in the *cox11* knockout strain. Por1p levels in these samples were indistinguishable from that of the wild-type strain (Fig. 4C). We noticed that while the levels of Cox2p and Cox3p were reduced, they were comparatively stronger than the signal for Cox1p. Densitometric analysis of band intensities from the aW303ΔCOX11 mitochondria

revealed that the residual levels of Cox2p and Cox3p were 19% and 50% of the wild-type level. However, the level of Cox1p was only 3% of that of the wild-type level. This is consistent with a recent report that demonstrated that translation of Cox1p is hindered in most COX assembly null mutants (2). However, the Y192R and V226W mutants (group 2, above) also had selectively reduced steady-state levels of Cox1p (Fig. 4D). Densitometric analysis of the V226W mutant demonstrated residual protein levels of 34%, 47%, and 46% for

Cox1p, Cox2p, and Cox3p, respectively. Similarly, the Y192R mutant also had a 10% lower amount of detectable Cox1p than Cox2p or Cox3p. This is reminiscent of our findings with *cox17* and *sco1* point mutants, in which there was a proportional restoration of Cox1p and Cox3p, but not of Cox2p (6, 22). This selective reduction in the level of subunit 1 protein is therefore the first in vivo support for a specific effect on the proposed acceptor site for the copper donated by Cox11p.

Given that a subset of *cox11* mutants had characteristics similar to those seen with the knockout strain, we wanted to determine the effect of the mutations on the steady-state levels of the Cox11 protein itself. Several of the *cox11* alleles with a null mutant phenotype—C208A, F209A, C210A, P225R—had reduced or undetectable levels of Cox11p (Fig. 4B) in the aW303ΔCOX11 background, while levels of Por1p appeared to be equivalent to that seen in the wild-type strain (Fig. 4C). Results obtained in the BY4741 genetic background, in which the same C208-C210 alleles were introduced into a Δ*cox11* mutant strain, resulted in expression of stable Cox11 protein (4), suggesting that the genetic background likely has an important influence on Cox11p stability. In contrast, the C111A and K205E alleles, which displayed a phenotype similar to that seen with C208A and C210A, had levels of Cox11p that were similar to those seen in respiratory competent W303 (Fig. 4B). Not surprisingly, all of the alleles with a wild-type or partially reduced rate of growth on EG had normal steady-state levels of Cox11p. We also observed stable, wild-type levels of Cox11p in the two strains (Y192R, V226W) with complete respiratory deficiency and a misassembled COX enzyme (Fig. 4D). These results suggest that the phenotypes of the Y192R and V226W mutants are not merely the result of a misfolded Cox11 protein but rather the result of occlusion of the surface pocket. In this regard, it is interesting that we observed that both Y192R and V226W produced spontaneous extragenic revertants at high frequency. However, we also noted that a C-terminal FLAG tag reduced this reversion rate substantially (data not shown), suggesting the existence of a physical interaction between Cox11p and another, as-yet-unidentified, protein.

The Cox11p matrix domain is resistant to deletion mutations. As mentioned above, there is virtually no evolutionary conservation of residues in the N-terminal one-third of the Cox11 protein, leading us to question whether this domain has an influence on Cox11p function. An interaction between the matrix tail of Cox11p and a subunit of the mitoribosome, MrpL36p, was recently reported (16). In addition, a domain swap experiment between Sco1p and Cox11p suggested a lack of specificity in the N-terminal domain of Cox11p (5). In order to determine if the matrix domain is important for Cox11p function, we generated sequential deletions along the length of the matrix domain, between the predicted matrix-processing peptidase (MPP) cleavage site and the predicted TM helix (Fig. 1). If an interaction between Cox11p and MrpL36p is important for Cox11p function in COX assembly, loss of an interaction domain should manifest in a respiration-deficient phenotype. Seven sequential five-amino-acid deletions, spanning residues 49 through 84, were generated, and each allele complemented the aW303ΔCOX11 strain, supporting growth on EG at the wild-type rate (Table 2). Subsequently, four separate sequential 10-amino-acid deletions were generated,

including one (Δ44-53) that removed the predicted MPP cleavage site (Fig. 1). As shown in Table 2, each of these four alleles was also fully capable of complementing the *cox11* null strain. These results suggest either that any interaction with the mitoribosome is not essential for Cox11p function or that the putative interaction domain was not perturbed in our set of deletion alleles. Removal of a further five residues into the predicted TM helix (Δ84-88) resulted in loss of Cox11p stability (Fig. 4B) and therefore a respiration-deficient phenotype similar to that seen in aW303ΔCOX11 (Table 2). This mutation likely abrogates correct membrane insertion of Cox11p, thus resulting in proteolytic degradation.

Δ*cox11* mutant strains are hydrogen peroxide hypersensitive. We previously reported that a yeast *sco1* null mutant has a hydrogen peroxide-hypersensitive phenotype (30). This observation, in the context of the crystal structure of hSCO1, has led to the proposal that Sco1p may have a second, previously unanticipated, function. Both Cox11p and Sco1p are copper-binding proteins of the inner mitochondrial membrane, and both are proposed to participate in similar pathways, namely, copper acquisition from Cox17p and copper donation to Cox1p and Cox2p, respectively. In light of this, we wanted to determine whether *cox11* mutants might display a similar hypersensitivity to hydrogen peroxide. We subjected the *cox11* null allele to acute hydrogen peroxide exposure and analyzed the effects of this exposure on the viability of the strain. As shown in Fig. 5, hydrogen peroxide had virtually no effect on the survival of wild-type aW303 cells. In contrast, the same treatment resulted in almost complete loss of viability of aW303ΔCOX11 cells. This hypersensitivity is clearly the result of loss of Cox11p, as a CEN plasmid-borne copy of *COX11* rescued aW303ΔCOX11 from the peroxide-sensitive phenotype (Fig. 5). This result was similar to that obtained with the aW303ΔSCO1 strain that we reported earlier (30). Loss of COX assembly alone, such as that resulting from loss of Cox4p (aW303ΔCOX4), Cox6p (aW303ΔCOX6), or Cox9p (aW303-ΔCOX9), does not result in peroxide sensitivity (Fig. 5), suggesting that peroxide sensitivity is not merely a consequence of the loss of assembled COX. In addition, a ρ⁰ derivative of W303 was also not peroxide sensitive (Fig. 5). It is interesting that a strain lacking Cox17p, which is proposed to be the copper donor for both Cox11p and Sco1p, also fails to demonstrate any hypersensitivity to hydrogen peroxide (Fig. 5). Taken together, these results demonstrate that Cox11p, and not respiration per se, is required for the cell to mount a response to acute peroxide exposure. These results are in contrast to previous studies, albeit with different strains, which indicated that COX and mitochondrial DNA are required for resistance to H_2O_2 (11, 14).

Given the hypersensitivity of the *cox11* null mutant to hydrogen peroxide, we wondered whether there might be an elevated level of oxidative stress associated with the loss of Cox11p and thus hypersensitivity to other radical-generating compounds. To that end, we tested the aW303ΔCOX11 strain for sensitivity to several free-radical-generating agents, including *t*-butyl hydroperoxide, paraquat, sodium nitroprusside, *N*-nitroso-diethylamine, 8-hydroxyquinoline, and nitroglycerin. None of these compounds appeared to have any effect on the viability of the *cox11* null strain (data not shown). Our results suggest a possible role for Cox11p (and
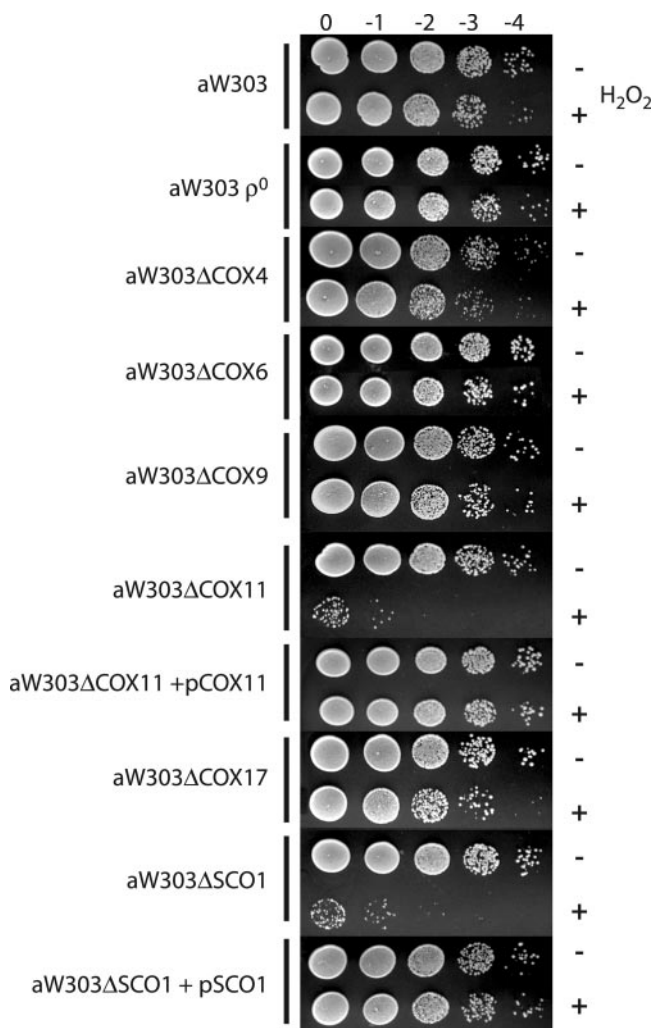
FIG. 5. The Δ*cox11* mutant is hypersensitive to hydrogen peroxide. Exponential-phase liquid cultures were exposed to 6 mM H_2O_2 (+) for 2 h, serially diluted, and spotted onto 1% yeast extract–2% peptone–2% dextrose plates along with untreated controls (−) and allowed to grow for 36 to 48 h to determine colony-forming potential. The W303 parent strain and the COX mutants aW303ΔCOX4, aW303ΔCOX6, aW303ΔCOX9, and aW303ΔCOX17, in addition to aW303 ρ^0, do not display sensitivity to H_2O_2, suggesting that loss of COX itself does not impart a peroxide-sensitive phenotype. aW303ΔCOX11 and aW303ΔSCO1 are hypersensitive to H_2O_2, and this phenotype can be rescued by expression of *COX11* and *SCO1*, respectively, from a low-copy-number plasmid.

Sco1p) in the response to oxidative stress induced by hydrogen peroxide.

DISCUSSION

The current model for copper acquisition by COX posits that Cox11p receives copper from Cox17p and inserts the metal into the Cu$_B$ site of Cox1p during COX assembly (13). Consistent with this model, Cox11p has been shown to bind copper and mutation of residues that abrogate the copper-binding ability of Cox11p result in a loss of functional COX (4). The recently published nuclear magnetic resonance (NMR) structure of *S. meliloti* Cox11 shows a protein that is almost

exclusively β-strands and loops, which form a barrel-like structure with extensive hydrogen bonding within the central core (1). Comparison of an alignment of multiple Cox11 proteins from a wide variety of species with the NMR structure reveals that the majority of the conserved residue side chains face the inside of the barrel-like structure, resulting in regions of identity at alternating residues along a β-strand.

We have characterized a large number of random and site-directed mutants in order to learn more about which conserved residues of Cox11p are important for its function. As part of this study, we mutagenized 19 conserved residues within the IMS domain of Cox11p, including the four that make up the CFCF copper-binding loop and 13 other IMS residues within β-strands. Surprisingly, we found that many of these residues tolerated significant amino acid changes despite the fact that they are absolutely conserved over evolution. This tolerance may be a result of the extensive hydrogen bonding within the core of Cox11p, such that a single change within the core may not be sufficient to destabilize folding. Three of the mutations that had a measurable impact on Cox11p function, as judged by a reduced ability to grow on a nonfermentable carbon source, were found in residues at the ends of β-strands. Residue N180 is in the interior of Cox11p, at the top of the molecule, whereas P225 and D231 are both on the exterior of Cox11p. We also identified a synthetic interaction between residues L106 and S150. The NMR structure of *S. meliloti* Cox11 shows no connection between these residues, and thus the reason for the complete respiratory deficiency of the L106P/S150P allele is not clear.

Another set of mutants with impaired Cox11p function contained mutations in residues lining the surface pocket behind the copper-binding loop, which we identified from the *S. meliloti* Cox11 structure. Both the Y192R and V226W mutations introduced a bulky side chain projecting into the center of this pocket, completely abrogating Cox11p function. Given that each of these alleles produced nearly normal steady-state levels of Cox11p, it seems unlikely that these mutant proteins have folded incorrectly, as misfolded proteins are generally subject to proteolytic degradation. In addition, mutation of the L248 and Y250 residues, which also line the interior of the pocket, resulted in partial respiratory deficiency. These results thus suggest that this pocket is important for Cox11p function, perhaps in forming a binding site for another molecule or protein. Though this pocket seems suitable for a small molecule, its identity is unknown.

Several of the alleles that were generated resulted in unstable Cox11p molecules when expressed in the W303 genetic background. These residues were typically on the exterior of Cox11p, with three of these (C208A, F209A, and C210A) being within the unstructured copper-binding loop. These three alleles were previously reported to be stable when expressed in BY4741 (4), suggesting the presence of a modifier locus that affects protein stability in one of these genetic backgrounds. Further study of these mutants may lead to an improved understanding of the factors impacting Cox11p stability in the different strain backgrounds. It may also identify proteins that have indirect effects on COX assembly.

The structure of *S. meliloti* Cox11 does not provide any information on either the matrix tail or TM domain of Cox11p. A recent report has suggested that the matrix domain is not

essential for Cox11p function (5). Our analysis of N-terminal deletion mutants supports the proposal that the matrix domain does not have an essential function in Cox11p, as none of our 5- or 10-amino-acid deletions resulted in a respiration-deficient phenotype. A further deletion (Δ84-88) into the matrix side of the predicted Cox11p TM domain destabilized the protein, resulting in complete respiratory deficiency. A recent report has also shown that replacement of the matrix and TM domains of Cox11p with those of Sco1p results in failure to complement Δ*cox11*, even though the chimeric protein is correctly targeted to the IMM (16). These results suggest that the Cox11p TM domain is essential for function beyond simple IMM targeting. It seems possible that the TM domain plays a role in stabilizing the Cox11p dimer, perhaps in conjunction with C111, the residue that is proposed to form a disulfide bridge involved in protein dimerization and is located in the IMS immediately adjacent to the inner membrane. A C111A mutant had complete loss of COX assembly, although Cox11p itself was stably expressed in the C111A mutant, in contrast with the degradation of Δ84-88 Cox11p. In this respect, the L106P mutation, which is immediately adjacent to the TM domain, also had a significant impact on Cox11p function.

Our characterization has also revealed a phenotype that has not hitherto been observed in yeast mutants, involving a partially active COX enzyme that is nonetheless misassembled. The shift in the cytochrome aa_3 peak indicates that hemes a and a_3 are in an abnormal environment. While other yeast COX assembly mutants described thus far have had a complete absence of COX activity in conjunction with a shift in the spectral peak, there are numerous descriptions of partially active and misassembled COX enzyme in studies with *Paracoccus denitrificans* mutants (15, 23). Our results therefore represent the first such mutants identified in yeast. Alternately, our analyses may indicate that there is a mixed population of COX molecules in the mitochondria of these mutants—some correctly assembled a COX enzyme that is fully active and some incorrectly assembled a COX enzyme that is inactive. Further examination of the COX enzymes found in these mutants should allow us to resolve this issue. In addition to demonstrating an altered heme environment in a subset of the *cox11* mutants, our studies provide the first evidence for a direct effect of Cox11p on its presumptive target, Cox1p, in a eukaryotic system. Our finding of a selective reduction of Cox1p in our *cox11* mutants parallels our findings of a selective reduction of Cox2p with our *sco1* and *cox17* mutants, in which there was a proportional restoration of Cox1p and Cox3p (6, 22). Although Cox1p translation is reduced in most COX assembly null mutants (2), our analysis with point mutants suggests that Cox1p may be proportionally more affected by mutant Cox11p. Our previous work with *sco1* and *cox17* has shown that point mutants are biochemically distinct from the null alleles, particularly as they are able to at least partially complete COX assembly (6, 22). These *cox11* mutants therefore represent an important resource in our attempts to delineate the mechanistic and temporal determinants of the COX assembly pathway.

In addition to identifying an interesting COX assembly phenotype among our *cox11* mutants, we have also identified a peroxide hypersensitivity in these mutants that is similar to that seen in Δ*sco1* mutant yeast (30). Although we tested a variety of COX assembly mutants against a range of nitrogen and oxygen radical-generating compounds, we only observed sensitivity in two strains, Δ*sco1* and Δ*cox11* mutants, to a single agent—hydrogen peroxide. Both strains displayed a hypersensitivity phenotype when challenged with H_2O_2 during the exponential growth phase. This peroxide hypersensitivity appears to be linked to the functionality of the Cox11p molecule, as those mutants with only a partial respiratory deficiency proved insensitive to peroxide (data not shown), suggesting that even partially functional Cox11p (with respect to COX assembly) can fully protect against peroxide exposure. It is intriguing that Δ*cox17* is not peroxide sensitive, especially in light of the current model of Cox17p as a copper donor to both Sco1p and Cox11p, suggesting that the absence of copper in COX alone does not underlie the phenotype. The insensitivity of all other COX mutants to peroxide further suggests that loss of COX holoenzyme assembly itself is also not a prerequisite for peroxide sensitivity. In light of the fact that aconitase is an extremely sensitive marker of oxidative stress, particularly with respect to H_2O_2 (3, 29), we are currently measuring aconitase activity in our *cox11* mutants.

Previous reports have shown that *cox11* is allelic to *pso7*, a mutation sensitive to photoactivated psoralens (19) and other mutagens activated by metabolism (20). However, in the W303 background used in our studies, we did not observe sensitivity to 8-hydroxyquinoline or *N*-nitroso-diethylamine, which had been previously observed in *cox11* mutants (20). Similar to our observation of the lack of peroxide sensitivity in Δ*cox6* and ρ^0 yeast, and the lack of Cox11p stability with several of our *cox11* alleles, the genetic background may play a currently underappreciated role in these phenotypes and it seems prudent to use diploid strains for future studies. Our results therefore suggest a possible role for Cox11p (and Sco1p) in mitochondrial redox balance, but how Cox11p fits into the larger cellular network associated with oxidative stress is not clear. Cox11p may be acting as a mitochondrial peroxidase, in a fashion similar to catalase (*CTA1*). However, overexpression of Cox11p does not confer increased resistance to hydrogen peroxide on W303, the wild-type parent strain (data not shown), arguing against a straightforward role for Cox11p as a peroxidase. Alternately, Cox11p may be acting to reverse peroxide-induced damage to COX. Further study of the Cox11 molecule will help to delineate the precise role of Cox11p in redox metabolism and COX assembly.

REFERENCES

1. **Banci, L., I. Bertini, F. Cantini, S. Ciofi-Baffoni, L. Gonnelli, and S. Mangani.** 2004. Solution structure of Cox11, a novel type of β-immunoglobulin-like fold involved in Cu$_B$ site formation of cytochrome *c* oxidase. J. Biol. Chem. **279:**34833–34839.
2. **Barrientos, A., A. Zambrano, and A. Tzagoloff.** 2004. Mss51p and Cox14p jointly regulate mitochondrial Cox1p expression in *Saccharomyces cerevisiae*. EMBO J. **23:**3472–3482.

3. **Brazzolotto, X., J. Gaillard, K. Pantopoulos, M. W. Hentze, and J. M. Moulis.** 1999. Human cytoplasmic aconitase (iron regulatory protein 1) is converted into its [3Fe-4S] form by hydrogen peroxide *in vitro* but is not activated for iron-responsive element binding. J. Biol. Chem. **274:**21625–21630.

4. **Carr, H. S., G. N. George, and D. R. Winge.** 2002. Yeast Cox11, a protein essential for cytochrome *c* oxidase assembly, is a Cu(I)-binding protein. J. Biol. Chem. **277:**31237–31242.

5. **Carr, H. S., A. B. Maxfield, Y.-C. Horng, and D. R. Winge.** 2005. Functional analysis of the domains in Cox11. J. Biol. Chem. **280:**22664–22669.

6. **Dickinson, E. K., D. L. Adams, E. A. Schon, and D. M. Glerum.** 2000. A human *SCO2* mutation helps define the role of Sco1p in the cytochrome oxidase assembly pathway. J. Biol. Chem. **275:**26780–26785.

7. **Glerum, D. M., A. Shtanko, and A. Tzagoloff.** 1996. Characterization of *COX17*, a yeast gene involved in copper metabolism and assembly of cytochrome oxidase. J. Biol. Chem. **271:**14504–14509.

8. **Glerum, D. M., A. Shtanko, and A. Tzagoloff.** 1996. *SCO1* and *SCO2* act as high copy suppressors of a mitochondrial copper recruitment defect in *Saccharomyces cerevisiae.* J. Biol. Chem. **271:**20531–20535.

9. **Glerum, D. M., and A. Tzagoloff.** 1998. Affinity purification of yeast cytochrome oxidase with biotinylated subunits 4, 5, or 6. Anal. Biochem. **260:**38–43.

10. **Goldring, E. S., L. I. Grossman, D. Krupnick, D. R. Cryer, and J. Marmur.** 1970. The petite mutation in yeast. Loss of mitochondrial deoxyribonucleic acid during induction of petites with ethidium bromide. J. Mol. Biol. **52:**323–335.

11. **Grant, C. M., F. H. MacIver, and I. W. Dawes.** 1997. Mitochondrial function is required for resistance to oxidative stress in the yeast *Saccharomyces cerevisiae.* FEBS Lett. **410:**219–222.

12. **Hiser, L., M. Di Valentin, A. G. Hamer, and J. P. Hosler.** 2000. Cox11p is required for stable formation of the Cu_B and magnesium centers of cytochrome *c* oxidase. J. Biol. Chem. **275:**619–623.

13. **Horng, Y.-C., P. A. Cobine, A. B. Maxfield, H. S. Carr, and D. R. Winge.** 2004. Specific copper transfer from the Cox17 metallochaperone to both Sco1 and Cox11 in the assembly of yeast cytochrome *c* oxidase. J. Biol. Chem. **279:**35334–35340.

14. **Jamieson, D. J.** 1998. Oxidative stress responses of the yeast *Saccharomyces cerevisiae.* Yeast **14:**1511–1527.

15. **Kannt, A., U. Pfitzner, M. Ruitenberg, P. Hellwig, B. Ludwig, W. Mantele, K. Fendler, and H. Michel.** 1999. Mutation of Arg-54 strongly influences heme composition and rate and directionality of electron transfer in *Paracoccus denitrificans* cytochrome *c* oxidase. J. Biol. Chem. **274:**37974–37981.

16. **Khalimonchuk, O., K. Ostermann, and G. Rodel.** 2005. Evidence for the association of yeast mitochondrial ribosomes with Cox11p, a protein required for the Cu_B site formation of cytochrome *c* oxidase. Curr. Genet. **47:**223–233.

17. **McEwen, J. E., C. Ko, B. Kloeckner-Gruissem, and R. O. Poyton.** 1986. Nuclear functions required for cytochrome *c* oxidase biogenesis in *Saccharomyces cerevisiae.* Characterization of mutants in 34 complementation groups. J. Biol. Chem. **261:**11872–11879.

18. **Nittis, T., G. N. George, and D. R. Winge.** 2001. Yeast Sco1, a protein essential for cytochrome *c* oxidase function is a Cu(I)-binding protein. J. Biol. Chem. **276:**42520–42526.

19. **Pungartnik, C., M. F. Kern, M. Brendel, and J. A. Henriques.** 1999. Mutant allele *pso7-1*, that sensitizes *Saccharomyces cerevisiae* to photoactivated psoralen, is allelic with *COX11*, encoding a protein indispensable for a functional cytochrome *c* oxidase. Curr. Genet. **36:**124–129.

20. **Pungartnik, C., J. Picada, M. Brendel, and J. A. Henriques.** 2002. Further phenotypic characterization of *pso* mutants of *Saccharomyces cerevisiae* with respect to DNA repair and response to oxidative stress. Genet. Mol. Res. **1:**79–89.

21. **Punter, F. A., and D. M. Glerum.** 2004. Defects in assembly of cytochrome oxidase: roles in mitochondrial disease, p. 123–148. *In* M. Koehler and M. F. Bauer (ed.), Topics in current genetics, vol. 8. Springer-Verlag, Heidelberg, Germany.

22. **Punter, F. A., and D. M. Glerum.** 2003. Mutagenesis reveals a specific role for Cox17p in copper transport to cytochrome oxidase. J. Biol. Chem. **278:**30875–30880.

23. **Riistama, S., M. I. Verkhovsky, L. Laakkonen, M. Wikstrom, and A. Puustinen.** 2000. Interaction between the formyl group of heme a and arginine 54 in cytochrome aa_3 from *Paracoccus denitrificans.* Biochim. Biophys. Acta **1456:**1–4.

24. **Schiestl, R. H., and R. D. Gietz.** 1989. High efficiency transformation of intact yeast cells using single stranded nucleic acids as a carrier. Curr. Genet. **16:**339–346.

25. **Srinivasan, C., M. C. Posewitz, G. N. George, and D. R. Winge.** 1998. Characterization of the copper chaperone Cox17 of *Saccharomyces cerevisiae.* Biochemistry **37:**7572–7577.

26. **Tsukihara, T., H. Aoyama, E. Yamashita, T. Tomizaki, H. Yamaguchi, K. Shinzawa-Itoh, R. Nakashima, R. Yaono, and S. Yoshikawa.** 1996. The whole structure of the 13-subunit oxidized cytochrome *c* oxidase at 2.8 Å. Science **272:**1136–1144.

27. **Tzagoloff, A., N. Capitano, M. P. Nobrega, and D. Gatti.** 1990. Cytochrome oxidase assembly in yeast requires the product of *COX11*, a homolog of the *P. denitrificans* protein encoded by ORF3. EMBO J. **9:**2759–2764.

28. **Tzagoloff, A., and C. L. Dieckmann.** 1990. *PET* genes of *Saccharomyces cerevisiae.* Microbiol. Rev. **54:**211–225.

29. **Vasquez-Vivar, J., B. Kalyanaraman, and M. C. Kennedy.** 2000. Mitochondrial aconitase is a source of hydroxyl radical. An electron spin resonance investigation. J. Biol. Chem. **275:**14064–14069.

30. **Williams, J. C., C. Sue, G. S. Banting, H. Yang, D. M. Glerum, W. A. Hendrickson, and E. A. Schon.** 2005. Crystal structure of human SCO1: implications for redox signaling by a mitochondrial cytochrome *c* oxidase "assembly" protein. J. Biol. Chem. **280:**15202–15211.